ELSEVIER

Physica A 288 (2000) 280–307

PHYSICA A

www.elsevier.com/locate/physa

Anomalous scaling in anisotropic turbulence

Itai Arad, Victor S. L'vov, Itamar Procaccia*

Department of Chemical Physics, The Weizmann Institute of Science, Rehovot 76100, Israel

Abstract

We present a short review of the work conducted by our group on the subject of anomalous scaling in anisotropic turbulence. The basic idea that unifies all the applications discussed here is that the equations of motion for correlation functions are always linear and invariant to rotations, and therefore the solutions foliate into sectors of the symmetry group of all rotations (SO(3)). We have considered models of passive scalar and passive vector advections by a rapidly changing turbulent velocity field (Kraichnan-type models) for which we find a discrete spectrum of universal anomalous exponents, with a different exponent characterizing the scaling behavior in every sector. Generically the correlation functions and structure functions appear as sums over all these contributions, with nonuniversal amplitudes which are determined by the anisotropic boundary conditions. In addition we considered Navier–Stokes turbulence by analyzing simulations and experiments, and reached some interesting conclusions regarding the scaling exponents in the anisotropic sectors. The theory presented here clarifies questions like the restoration of local isotropy upon decreasing scales. We explain when the local isotropy is fully restored and when the lingering effects of the anisotropic forcing appear for arbitrarily small scales.

1. Introduction

In this paper we review some recent work aimed at understanding the effects of anisotropy on the universal aspects of scaling behaviour in turbulent systems. We have shown recently [1] that in the presence of anisotropic effects (which are ubiquitous in realistic turbulent systems) one needs to carefully disentangle the various universal scaling contributions. Even at the largest available Reynolds numbers the observed scaling behavior is not simple, being composed of several contributions with different scaling exponents. The statistical objects like structure functions and correlation functions are characterized by one leading scaling (or homogeneity) exponent only in the idealized case of full isotropy, or infinite Reynolds numbers when the scaling regime

* Corresponding author.

E-mail address: cfprocac@weizmann.weizmann.ac.il (I. Procaccia).

0378-4371/00/$ - see front matter
PII: S0378-4371(00)00427-1

is of infinite extent. Anisotropy results in mixing of various contributions to the statistical objects, each of which is characterized by one leading universal exponent, but the total is a sum of such contributions which appears not to “scale” in standard log–log plots. By realizing that the correlation functions have natural projections on the irreducible representations of the SO(3) symmetry group we could offer methods of data analysis [2–4] that allow one to measure the universal scaling exponents in each sector separately. From the theoretical point of view we need to understand how the existence of anisotropy gives rise to new families of universal scaling exponents which were traditionally not considered. The relative importance of the contributions of the various sectors of the symmetry group are determined by the boundary conditions, and therefore are not universal.

In addition to Navier–Stokes turbulence, we consider passive scalar [5] and passive vector [6] turbulent advection. In the latter case, one can offer satisfactory understanding of the physics of anomalous scaling in the isotropic [6–9] as well as in the anisotropic sectors [10–14]. We therefore, dedicate some space in the next section to the discussion of the connection between Lagrangian trajectories and the statistics of advected fields [15–18]. This connection provides a very clear understanding of the physical origin of the anomalous exponents, relating them to the dynamics in the space of *shapes* of groups of Lagrangian paths. In Section 3 we review the actual calculation of the spectrum of the anomalous exponents in all the sectors of the symmetry group for the case of Kraichnan’s model of passive scalar advection [13]. This example, as all the others, underlies the importance of identifying the appropriate irreducible representations of the SO(3) symmetry group. Once this is done the calculations become relatively straightforward. In Section 4 we review briefly the case of passive vector advection, in which the anomalous exponents of the second-order structure functions can be computed exactly in all the sectors of the symmetry group. This tensorial correlation calls for tensorial irreducible representations differing from the cases of passive scalars.

It is noteworthy that for both passive and vector scalar advection the foliation in terms of sectors of the rotation group can be exactly proven, each sector being characterized by an index ℓ, m, and a family of exponents which are m-independent. One of the important results of the analysis is that the over all spectrum of anomalous exponents is discrete and is a strictly increasing function of ℓ. This is important, since it shows that for any quantity that has an isotropic component, for diminishing scales the higher-order scaling exponents become irrelevant, and for sufficiently small scales only the isotropic contribution survives. As the scaling exponents ζ appear in power laws of the type $(R/L)^{\zeta}$, with L being some typical outer scale and $R \ll L$, the larger is the exponent, the faster is the decay of the contribution as the scale R diminishes. This is precisely how the isotropization of the small scales takes place, and the higher order exponents describe the rate of isotropization.

In Section 5 we turn to the analysis of Navier–Stokes turbulence and discuss simulations and experiments from which we extract information about the scaling exponents in the higher sectors of the symmetry group. Some of the open questions and the road ahead will be presented in Section 6.

2. Anisotropy and scaling in the Kraichnan model of passive scalar advection

2.1. The model

The model of passive scalar advection with rapidly decorrelating velocity field was introduced by Kraichnan [5] as early as in 1968. In recent years [7,8] it was shown to be a fruitful case model for understanding multiscaling in the statistical description of turbulent fields. The basic dynamical equation in this model is for a scalar field $T(\boldsymbol{r},t)$ advected by a random velocity field $\boldsymbol{u}(\boldsymbol{r},t)$:

$$[\partial_t - \kappa_0\nabla^2 + \boldsymbol{u}(\boldsymbol{r},t)\cdot\boldsymbol{\nabla}]T(\boldsymbol{r},t) = f(\boldsymbol{r},t)\,. \tag{2.1}$$

In this equation $f(\boldsymbol{r},t)$ is the forcing and κ_0 is the molecular diffusivity. In Kraichnan's model the advecting field $\boldsymbol{u}(\boldsymbol{r},t)$ as well as the forcing field $f(\boldsymbol{r},t)$ are taken to be Gaussian, time and space homogeneous, and delta-correlated in time

$$\langle(u^\alpha(\boldsymbol{r},t) - u^\alpha(\boldsymbol{r}',t))(u^\beta(\boldsymbol{r},t') - u^\beta(\boldsymbol{r}',t'))\rangle_{\boldsymbol{u}} = h^{\alpha\beta}(\boldsymbol{r}-\boldsymbol{r}')\delta(t-t')\,, \tag{2.2}$$

where the "eddy-diffusivity" tensor $h^{\alpha\beta}(\boldsymbol{r})$ is defined by

$$h^{\alpha\beta}(\boldsymbol{r}) = D\left(\frac{r}{\Lambda}\right)^{\xi}\left(\delta^{\alpha\beta} - \frac{\xi}{d-1+\xi}\frac{r^\alpha r^\beta}{r^2}\right), \quad \eta \ll r \ll \Lambda\,. \tag{2.3}$$

Here η and Λ are the inner and outer scale for the velocity fields, D is a dimensional constant, and the coefficients are chosen such that $\partial_\alpha h^{\alpha\beta} = 0$. The averaging $\langle\ldots\rangle_{\boldsymbol{u}}$ is done with respect to the realizations of the velocity field. The forcing f is also taken white in time and Gaussian

$$\langle f(\boldsymbol{r},t) f(\boldsymbol{r}',t')\rangle_f = \Xi(\boldsymbol{r}-\boldsymbol{r}')\delta(t-t')\,. \tag{2.4}$$

Here the average is done with respect to realizations of the forcing. The forcing is taken to act only on the large scales, of the order of L (with a compact support in Fourier space). This means that the function $\Xi(r)$ is nearly constant for $r \ll L$ but it decays rapidly for $r > L$.

From the point of view of the statistical theory one is interested mostly in the scaling exponents characterizing the structure functions

$$S_{2n}(\boldsymbol{r}_1 - \boldsymbol{r}_2) = \langle(T(\boldsymbol{r}_1,t) - T(\boldsymbol{r}_2,t))^{2n}\rangle_{\boldsymbol{u},f}\,. \tag{2.5}$$

For isotropic forcing one expects S_{2n} to depend only on the distance $R \equiv |\boldsymbol{r}_1 - \boldsymbol{r}_2|$ such that in the scaling regime

$$S_{2n}(R) \propto R^{\zeta_{2n}} \propto [S_2(R)]^n \left(\frac{L}{R}\right)^{\delta_{2n}}\,. \tag{2.6}$$

In this equation we introduced the "normal" ($n\zeta_2$) and the anomalous (δ_{2n}) parts of the scaling exponents $\zeta_{2n} = n\zeta_2 - \delta_{2n}$. The first part can be obtained from dimensional considerations, but the anomalous part cannot be guessed from simple arguments.

When the forcing is anisotropic, the structure functions depend on the vector distance $\boldsymbol{R}=\boldsymbol{r}_1-\boldsymbol{r}_2$. In this case we can represent them in terms of spherical harmonics,

$$S_{2n}(\boldsymbol{R})=\sum_{\ell,m} a_{\ell,m}(R)Y_{\ell,m}(\hat{\boldsymbol{R}})\,, \tag{2.7}$$

where $\hat{\boldsymbol{R}}\equiv\boldsymbol{R}/R$. This is a case in which the statistical object is a scalar function of one vector, and the appropriate basis of irreducible representations of the SO(3) symmetry group are obvious. We are going to explain in the next section that the coefficients $a_{\ell,m}(R)$ are expected to scale with a leading scaling exponent $\zeta_{2n}^{(\ell)}$ which is ℓ dependent but not m dependent. In Section 4 we review some recent results about the actual calculation of these exponents.

2.2. Lagrangian trajectories, correlation functions and shape dynamics

Theoretically it is natural to consider correlation functions rather than structure functions. The $2n$-order correlation functions are defined as

$$F_{2n}(\boldsymbol{r}_1,\ldots,\boldsymbol{r}_{2n})\equiv\langle T(\boldsymbol{r}_1)T(\boldsymbol{r}_2)\ldots T(\boldsymbol{r}_{2n})\rangle_{\boldsymbol{u},f}\,. \tag{2.8}$$

For separations $r_{ij}\to 0$ ($r_{ij}\equiv|\boldsymbol{r}_i-\boldsymbol{r}_j|$) the correlation functions converge to $\langle T^{2n}\rangle_{f,u}$, whereas for $r_{ij}\to L$ decorrelation leads to convergence to $\langle T\rangle^n_{\boldsymbol{u},f}$. For all $r_{ij}\approx O(r)\ll L$ one expects a behavior according to

$$F_{2n}(\boldsymbol{r}_1,\ldots,\boldsymbol{r}_{2n})=L^{n(2-\xi)}\left(c_0+\cdots+c_k(r/L)^{\zeta_{2n}}\tilde{F}_{2n}(\tilde{\boldsymbol{r}}_1,\ldots,\tilde{\boldsymbol{r}}_{2n})+\cdots\right)\,, \tag{2.9}$$

where $\tilde{F}_{2n}$ is a scaling function depending on $\tilde{\boldsymbol{r}}_i$ which denotes a set of dimensionless coordinates describing the configuration of the $2n$ points. The exponents and scaling functions are expected to be universal, but not the c coefficients, which depend on the details of forcing.

It has been shown [7,8] that the anomalous exponents ζ_{2n} can be obtained by finding the zero modes of the exact differential equations which are satisfied by F_{2n}. The equations for the zero modes read

$$\left[-\kappa\sum_i\nabla_i^2+\hat{\mathscr{B}}_{2n}\right]F_{2n}(\boldsymbol{r}_1,\boldsymbol{r}_2,\ldots,\boldsymbol{r}_{2n})=0 \tag{2.10}$$

and are obtained simply by omitting the nonhomogeneous part of the differential equations for F_{2n} [5]. The operator $\hat{\mathscr{B}}_{2n}\equiv\sum_{i>j}^{2n}\hat{\mathscr{B}}_{ij}$, and $\hat{\mathscr{B}}_{ij}$ are defined by

$$\hat{\mathscr{B}}_{ij}\equiv\hat{\mathscr{B}}(\boldsymbol{r}_i,\boldsymbol{r}_j)=h^{\alpha\beta}(\boldsymbol{r}_i-\boldsymbol{r}_j)\partial^2/\partial r_i^\alpha\partial r_j^\beta\,. \tag{2.11}$$

We will come back to this equation in Subsect C.

A different approach to finding the correlation functions is furnished by Lagrangian dynamics [16–18]. In this formalism one recognizes that the actual value of the scalar at position $\boldsymbol{r}$ at time t is determined by the action of the forcing along the Lagrangian trajectory from $t=-\infty$ to t:

$$T(\boldsymbol{r}_0,t_0)=\int_{-\infty}^{t_0}\mathrm{d}t\langle f(\boldsymbol{r}(t),t)\rangle_{\tilde{\boldsymbol{\eta}}} \tag{2.12}$$

with the trajectory $\boldsymbol{r}(t)$ obeying

$$\boldsymbol{r}(t_0) = \boldsymbol{r}_0 ,$$

$$\partial_t \boldsymbol{r}(t) = \boldsymbol{u}(\boldsymbol{r}(t), t) + \sqrt{2\kappa}\tilde{\boldsymbol{\eta}}(t) \tag{2.13}$$

and $\boldsymbol{\eta}$ is a vector of zero-mean independent Gaussian white random variables, $\langle \tilde{\eta}^\alpha(t)\tilde{\eta}^\beta(t')\rangle = \delta^{\alpha\beta}\delta(t-t')$. $\tilde{\boldsymbol{\eta}}$ role is to account for the dissipation of $T(\boldsymbol{r},t)$ in (2.1) [17]. With this in mind, we can rewrite F_{2n} by substituting each factor of $T(\boldsymbol{r}_i)$ by its representation (2.12). Performing the averages over the random forces, we end up with

$$F_{2n}(\boldsymbol{r}_1,\dots,\boldsymbol{r}_{2n},t_0) = \left\langle \int_{-\infty}^{t_0} \mathrm{d}t_1 \cdots \mathrm{d}t_n \, [\Xi(\boldsymbol{r}_1(t_1) - \boldsymbol{r}_2(t_1)) \times \cdots \times \Xi(\boldsymbol{r}_{2n-1}(t_n) - \boldsymbol{r}_{2n}(t_n)) + \text{ permutations}] \right\rangle_{\boldsymbol{u},\{\tilde{\boldsymbol{\eta}}_i\}} \tag{2.14}$$

To understand the averaging procedure recall that each of the trajectories $\boldsymbol{r}_i$ obeys an equation of form (2.13), where $\boldsymbol{u}$ as well as $\{\tilde{\boldsymbol{\eta}}_i\}_{i=1}^{2n}$ are independent stochastic variables whose correlations are given above.

In considering Lagrangian trajectories of *groups* of particles, we note that every configuration of $2n$ particles is characterized by a *center of mass*, say $\boldsymbol{R}$, a *scale* s (say the radius of gyration of the cluster of particles) and a *shape* $\boldsymbol{Z}$. By "shape" we mean here all the degrees of freedom other than the scales and $\boldsymbol{R}$: as many angles as are needed to fully determine a shape, in addition to the Euler angles that fix the orientation with respect to a chosen frame of coordinates. Thus a group of $2n$ positions $\{\boldsymbol{r}_i\}$ will be sometimes denoted below as $\{\boldsymbol{R}, s, \boldsymbol{Z}\}$.

We now focus our attention to the dynamic of such configurations. An initial configuration of particles will exhibit a rescaling of all the distances which increase on the average like t^{1/ζ_2}; this rescaling is analogous to Richardson diffusion. The exponent ζ_2 which determines the scale increase is also the characteristic exponent of the second-order structure function [5]. This has been related to the exponent ξ of (2.3) according to $\zeta_2 = 2 - \xi$. After factoring out this overall expansion we are left with a normalized 'shape'. It is the evolution of this shape that determines the anomalous exponents.

To see that, let us consider a final shape $\boldsymbol{Z}_0$ with an overall scale s_0 which is realized at $t = 0$. This shape has evolved during negative times. We fix a scale $s > s_0$ and examine the shape when the configuration reaches the scale s for the last time before reaching the scale s_0. Since the trajectories are random, the shape $\boldsymbol{Z}$, which is realized at this time, is taken from a distribution $\gamma(\boldsymbol{Z}; \boldsymbol{Z}_0, s \to s_0)$. As long as the advecting velocity field is scale invariant, this distribution can depend only on the ratio s/s_0. We can use the shape-to-shape transition probability to define an operator $\hat{\gamma}(s/s_0)$ on the space of functions $\Psi(\boldsymbol{Z})$ according to

$$[\hat{\gamma}(s/s_0)\Psi](Z_0) \equiv \int \mathrm{d}\boldsymbol{Z}\gamma(\boldsymbol{Z}; \boldsymbol{Z}_0, s \to s_0)\Psi(\boldsymbol{Z}) . \tag{2.15}$$

We will be interested in the eigenfunction and eigenvalues of this operator. This operator has two important properties. First, for an isotropic statistics of the velocity field the operator is isotropic. This means that this operator commutes with all rotation operators on the space of functions $\Psi(\boldsymbol{Z})$. In other words, if $\mathcal{O}_\Lambda$ is the rotation operator that takes the function $\Psi(\boldsymbol{Z})$ to the new function $\Psi(\Lambda^{-1}\boldsymbol{Z})$, then

$$\mathcal{O}_\Lambda\hat{\gamma} = \hat{\gamma}\mathcal{O}_\Lambda \,. \tag{2.16}$$

This property follows from the obvious symmetry of the Kernel $\gamma(\boldsymbol{Z};\boldsymbol{Z}_0, s \to s_0)$ to rotating $\boldsymbol{Z}$ and $\boldsymbol{Z}_0$ simultaneously. Accordingly, the eigenfunctions of $\hat{\gamma}$ can be classified according to the irreducible representations of SO(3) symmetry group. We will denote these eigenfunctions as $B_{q\ell m}(\boldsymbol{Z})$. Here $\ell = 0, 1, 2, \ldots$, $m = -\ell, -\ell+1, \ldots \ell$ and q stands for the remaining degrees of freedom.

The second important property of $\hat{\gamma}$ follows from the δ-correlation in time of the velocity field, which implies for the kernel that

$$\gamma(\boldsymbol{Z};\boldsymbol{Z}_0, s \to s_0) = \int \mathrm{d}\boldsymbol{Z}_1\, \gamma(\boldsymbol{Z};\boldsymbol{Z}_1, s \to s_1)\gamma(\boldsymbol{Z}_1;\boldsymbol{Z}_0, s_1 \to s_0), \quad s > s_1 > s_0 \tag{2.17}$$

and in turn, for the operator, that

$$\hat{\gamma}(s/s_0) = \hat{\gamma}(s/s_1)\hat{\gamma}(s_1/s_0) \,. \tag{2.18}$$

Accordingly, by a successive application of $\hat{\gamma}(s/s_0)$ to an arbitrary eigenfunction, we get that the eigenvalues of $\hat{\gamma}$ have to be of the form $\alpha_{q,\ell} = (s/s_0)^{\zeta(q,\ell)}$:

$$\left(\frac{s}{s_0}\right)^{\zeta(q,\ell)} B_{q\ell m}(\boldsymbol{Z}_0) = \int \mathrm{d}\boldsymbol{Z}\gamma(\boldsymbol{Z};\boldsymbol{Z}_0, s \to s_0)B_{q\ell m}(\boldsymbol{Z}) \,. \tag{2.19}$$

Notice that the eigenvalues are not a function of m. This follows from Schur's lemmas [19], but can be also explained from the fact that the rotation operator mixes the different m's: Take an eigenfunction $B_{q\ell m}(\boldsymbol{Z})$, and act on it once with the operator $\mathcal{O}_\Lambda\hat{\gamma}(s/s_0)$ and once with the operator $\hat{\gamma}(s/s_0)\mathcal{O}_\Lambda$. By virtue of (2.16) we should get that same result, but this is only possible if all the eigenfunctions with the same ℓ *and* the same q share the same eigenvalue.

To proceed, we want to connect the correlation function at scale s_0 to the correlation function at scale $s > s_0$. This can be done by splitting the trajectories in (2.14) into a part where a scale is larger than s, and to a part where the scale is between s and s_0. To this aim consider any set of Lagrangian trajectories that started at $t = -\infty$ and end up at time $t = 0$ in a configuration characterized by a scale s_0 and center of mass $\boldsymbol{R}_0 = 0$. A full measure of these have evolved through the scale L or larger. Accordingly they must have passed, during their evolution from time $t = -\infty$ through a configuration of scale $s > s_0$ at least once. Denote now

$$\mu_{2n}(t, R, \boldsymbol{Z}; s \to s_0, \boldsymbol{Z}_0)\,\mathrm{d}t\,\mathrm{d}\boldsymbol{R}\,\mathrm{d}\boldsymbol{Z} \tag{2.20}$$

as the probability that this set of $2n$ trajectories crossed the scale s for the last time before reaching $s_0, \boldsymbol{Z}_0$, between t and $t + \mathrm{d}t$, with a center of mass between $\boldsymbol{R}$ and $\boldsymbol{R} + \mathrm{d}\boldsymbol{R}$ and with a shape between $\boldsymbol{Z}$ and $\boldsymbol{Z} + \mathrm{d}\boldsymbol{Z}$.

In terms of this probability we can rewrite Eq. (2.14) (displaying, for clarity, $\boldsymbol{R}_0 = 0$ and $t_0 = 0$) as

$$\begin{aligned} F_{2n}(\boldsymbol{R}_0 = 0, s_0, \boldsymbol{Z}_0, t_0 = 0) = & \int \mathrm{d}\boldsymbol{Z} \int_{-\infty}^{0} \mathrm{d}t \int \mathrm{d}\boldsymbol{R} \mu_{2n}(t, R, \boldsymbol{Z}; s \to s_0, \boldsymbol{Z}_0) \\ & \times \left\langle \int_{-\infty}^{0} \mathrm{d}t_1 \cdots \mathrm{d}t_n \, [\Xi(\boldsymbol{r}_1(t_1) - \boldsymbol{r}_2(t_1)) \cdots \Xi(\boldsymbol{r}_{2n-1}(t_n) \right. \\ & \left. - \boldsymbol{r}_{2n}(t_n)) + \text{ perms}] | \, (s; \boldsymbol{R}, \boldsymbol{Z}, t) \right\rangle_{\boldsymbol{u}, \tilde{\boldsymbol{\eta}}_i} . \end{aligned} \tag{2.21}$$

The meaning of the conditional averaging $\langle \ldots | (s; \boldsymbol{R}, \boldsymbol{Z}, t) \rangle_{\boldsymbol{u}, \tilde{\boldsymbol{\eta}}_i}$ is an averaging over all the realizations of the velocity field and the random $\boldsymbol{\eta}_i$, for which Lagrangian trajectories that ended up at time $t_0 = 0$ in $\boldsymbol{R} = 0, s_0, \boldsymbol{Z}_0$ passed through $\boldsymbol{R}, s, \boldsymbol{Z}$ at time t.

Next, the time integrations in Eq. (2.21) are split into the interval $[-\infty, t]$ and $[t, 0]$ giving rise to 2^n different contributions:

$$\int_{-\infty}^{t} \mathrm{d}t_1 \cdots \int_{-\infty}^{t} \mathrm{d}t_n + \int_{t}^{0} \mathrm{d}t_1 \int_{-\infty}^{t} \mathrm{d}t_2 \cdots \int_{-\infty}^{t} \mathrm{d}t_n + \cdots . \tag{2.22}$$

Consider first the contribution with n integrals in the domain $[-\infty, t]$. It follows from the delta-correlation in time of the velocity field, that we can write

$$\begin{aligned} & \left\langle \int_{-\infty}^{t} \mathrm{d}t_1 \cdots \mathrm{d}t_n \, [\Xi(\boldsymbol{r}_1(t_1) - \boldsymbol{r}_2(t_1)) \right. \\ & \quad \left. \cdots \Xi(\boldsymbol{r}_{2n-1}(t_n) - \boldsymbol{r}_{2n}(t_n)) + \text{perms}] | \, (s; \boldsymbol{R}, \boldsymbol{Z}, t) \right\rangle_{\boldsymbol{u}, \tilde{\boldsymbol{\eta}}_i} \\ & = \left\langle \int_{-\infty}^{t} \mathrm{d}t_1 \cdots \mathrm{d}t_n \left[\Xi(\boldsymbol{r}'_1(t_1) - \boldsymbol{r}'_2(t_1)) \cdots \Xi(\boldsymbol{r}'_{2n-1}(t_n) - \boldsymbol{r}'_{2n}(t_n)) + \text{perms} \right] \right\rangle_{\boldsymbol{u}, \tilde{\boldsymbol{\eta}}_i} \\ & = F_{2n}(\boldsymbol{R}, s, \boldsymbol{Z}, t) = F_{2n}(s, \boldsymbol{Z}) , \end{aligned} \tag{2.23}$$

where in the last average, the trajectories $\boldsymbol{r}'_i(\cdot)$ are defined by their end point at time t which is $(\boldsymbol{R}, s, \boldsymbol{Z})$. The last equality follows from translational invariance in space-time. Accordingly, the contribution with n integrals in the domain $[-\infty, t]$ can be written as

$$\int \mathrm{d}\boldsymbol{Z} \, F_{2n}(s, \boldsymbol{Z}) \int_{-\infty}^{0} \mathrm{d}t \int \mathrm{d}\boldsymbol{R} \, \mu_{2n}(t, R, \boldsymbol{Z}; s \to s_0, \boldsymbol{Z}_0) . \tag{2.24}$$

Identifying the shape-to-shape transition probability:

$$\gamma(\boldsymbol{Z};\boldsymbol{Z}_0,s\to s_0)=\int_{-\infty}^{0}\mathrm{d}t\int \mathrm{d}\boldsymbol{R}\,\mu_{2n}(t,R,\boldsymbol{Z};s\to s_0,\boldsymbol{Z}_0)\,. \tag{2.25}$$

We can write Eq. (2.22) as

$$F_{2n}(s_0,\boldsymbol{Z}_0)=I+\int \mathrm{d}\boldsymbol{Z}\,\gamma(\boldsymbol{Z};\boldsymbol{Z}_0,s\to s_0)F_{2n}(s,\boldsymbol{Z})\,. \tag{2.26}$$

Here I represents all the contributions with one or more time integrals in the domain $[t,0]$. The key point now is that only the term with n integrals in the domain $[-\infty,t]$ contains information about the evolution of $2n$ Lagrangian trajectories that probed the forcing scale L. Accordingly, the term denoted by I cannot contain information about the leading anomalous scaling exponent belonging to F_{2n}, but only of lower-order exponents. The anomalous scaling dependence of the LHS of Eq. (2.26) has to cancel against the integral containing F_{2n} without the intervention of I.

Representing now

$$F_{2n}(s_0,\boldsymbol{Z}_0)=\sum_{q\ell m}a_{q,\ell m}(s_0)B_{q\ell m}(\boldsymbol{Z}_0)\,,$$

$$F_{2n}(s,\boldsymbol{Z})=\sum_{q\ell m}a_{q,\ell m}(s)B_{q\ell m}(\boldsymbol{Z})\,,$$

$$I=\sum_{q\ell m}I_{q\ell m}B_{q\ell m}(\boldsymbol{Z}_0) \tag{2.27}$$

and substituting on both sides of Eq. (2.26) and using Eq. (2.19) we find, due to the linear independence of the eigenfunctions $B_{q\ell m}$

$$a_{q,\ell m}(s_0)=I_{q\ell m}+\left(\frac{s}{s_0}\right)^{\zeta_{q,\ell}}a_{q,\ell m}(s)\,. \tag{2.28}$$

Contribution of $I_{q\ell m}$ to the leading order is neglected, leading to the conclusion that *the spectrum of anomalous exponents of the correlation functions is determined by the eigenvalues of the shape-to-shape transition probability operator.*

2.3. Analytic calculation of the anomalous exponents in the higher sectors of the symmetry group

Analytic calculation of the scaling exponents in the higher sectors of the symmetry group are available only for small values of ξ, where ξ is the scaling exponent characterizing the velocity structure functions (cf. Eq. (2.3)). In Ref. [13] such calculations were presented to $O(\xi)$. Calculations to $O(\xi^2)$ and $O(\xi^3)$ are available and will be published in the near future [20]. To $O(\xi)$ one can do the calculation in a number of ways, either via the zero modes of Eq. (2.10) or via a calculation of the moments of ∇T. For the second and higher orders in ξ the calculations of the zero modes are currently not available, and the reader is advised to consult the calculations of moments of ∇T in Ref. [20]. Nevertheless, for the purposes of this short review it is enough to present the exponents to $O(\xi)$, and we opt for the zero mode approach which is more sleek.

We thus consider the zero-modes of Eq. (2.10). In other words, we seek solutions $F_{2n}(\{\boldsymbol{r}_m\})$ which in the inertial interval solve the homogeneous equation

$$\sum_{i\neq j=1}^{2n} h^{\alpha\beta}(\boldsymbol{r}_i-\boldsymbol{r}_j)\nabla_i^\alpha\nabla_j^\beta F_{2n}(\{\boldsymbol{r}_m\})=0\,. \tag{2.29}$$

We allow anisotropy on the large scales. Since as before all the operators here are isotropic and the equation is linear, the solution space foliate into sectors $\{\ell,m\}$ corresponding the irreducible representations of the SO(3) symmetry group. Accordingly, we write the solution in the form

$$F_{2n}(\{\boldsymbol{r}_m\})=\sum_{\ell m} F_{2n,\ell m}(\{\boldsymbol{r}_m\})\,, \tag{2.30}$$

where $F_{2n,\ell m}$ are functions that transform under rotations according to the (ℓ,m) sector of the irreducible representations of SO(3). (Note that in the context of the last section, these functions can be written as $F_{2n,\ell m}(\{\boldsymbol{r}_m\})=\sum_q a_{q,\ell,m}(s)B_{q\ell m}(\boldsymbol{Z})$.) Each of these components is now expanded in ξ. In other words, we write, in the notation of Ref. [21],

$$F_{2n,\ell m}=E_{2n,\ell m}+\xi G_{2n,\ell m}+O(\xi^2)\,. \tag{2.31}$$

For $\xi=0$ Eq. (2.29) simplifies to

$$\sum_{i=1}^{2n}\nabla_i^2 E_{2n,\ell m}(\{\boldsymbol{r}_m\})=0 \tag{2.32}$$

for any value of ℓ,m. Next, we expand the operator in Eq. (2.29) in ξ and collect the terms of $O(\xi)$:

$$\sum_{i=1}^{2n}\nabla_i^2 G_{2n,\ell m}(\{\boldsymbol{r}_m\})=V_{2n}E_{2n,\ell m}(\{\boldsymbol{r}_m\})\,, \tag{2.33}$$

where ξV_{2n} is the first-order term in the expansion of the operator in (2.29):

$$V_{2n}\equiv\sum_{j\neq k=1}^{2n}\left[\delta^{\alpha\beta}\log(r_{jk})-\frac{r_{jk}^\alpha r_{jk}^\beta}{2r_{jk}^2}\right]\nabla_j^\alpha\nabla_k^\beta \tag{2.34}$$

and $\boldsymbol{r}_{jk}\equiv\boldsymbol{r}_j-\boldsymbol{r}_k$.

In solving Eq. (2.32) we are led by the following considerations: we want scale-invariant solutions, which are powers of $\boldsymbol{r}_{jk}$. We want analytic solutions, and thus we are limited to polynomials. Finally, we want solutions that involve all the $2n$ coordinates for the function $E_{2n,\ell m}$; any part of the solution with fewer coordinates will not contribute to the structure functions (2.5). To see this note that the structure function is a linear combination of correlation functions. This linear combination can be represented in terms of the difference operator $\delta_j(\boldsymbol{r},\boldsymbol{r}')$ defined by

$$\delta_j(\boldsymbol{r},\boldsymbol{r}')F(\{\boldsymbol{r}_m\}) \equiv F(\{\boldsymbol{r}_m\})|_{\boldsymbol{r}_j=\boldsymbol{r}} - F(\{\boldsymbol{r}_m\})|_{\boldsymbol{r}_j=\boldsymbol{r}'} \,. \tag{2.35}$$

Then,

$$S_{2n}(\boldsymbol{r}_1,\boldsymbol{r}_2\ldots\boldsymbol{r}_{2n}\boldsymbol{r}'_{2n}) = \prod_j \delta_j(\boldsymbol{r}_j,\boldsymbol{r}'_j)F(\{\boldsymbol{r}_m\})\,. \tag{2.36}$$

Accordingly, if $F(\{\boldsymbol{r}_m\})$ does not depend on $\boldsymbol{r}_k$, then $\delta_k(\boldsymbol{r}_k,\boldsymbol{r}'_k)F(\{\boldsymbol{r}_m\})=0$ identically. Since the difference operators commute, we can have no contribution to the structure functions from parts of F_{2n} that depend on less than $2n$ coordinates. Finally, we want the minimal polynomial because higher-order ones are negligible in the limit $r_{jk} \ll \Lambda$. Accordingly, $E_{2n,\ell m}$ with $\ell \leqslant 2n$ is a polynomial of the order $2n$. Consulting the appendix for the irreducible representations of the SO(3) symmetry group, we can write the most general form of polynomial $E_{2n,\ell m}$, up to an arbitrary factor, as

$$E_{2n,\ell m} = r_1^{\alpha_1}\ldots r_{2n}^{\alpha_{2n}} B_{2n,\ell m}^{\alpha_1\ldots\alpha_{2n}} + [\ldots]\,, \tag{2.37}$$

where $[\ldots]$ stands for all the terms that contain less than $2n$ coordinates; these do not appear in the structure functions, but maintain the translational invariance of our quantities. The appearance of the tensor $B_{2n,\ell m}^{\alpha_1\ldots\alpha_n}$ of the appendix is justified by the fact that $E_{2n,\ell m}$ must be symmetric to permutations of any pair of coordinates on the one hand, and it has to belong to the ℓ,m sector on the other hand. This requires the appearance of the fully symmetric tensor (A.1).

In light of Eqs. (2.33) and (2.34) we seek solution for $G_{2n}^{(\ell)}(\{\boldsymbol{r}_m\})$ of the form

$$G_{2n,\ell m}(\{\boldsymbol{r}_m\}) = \sum_{j\neq k} H_{\ell m}^{jk}(\{\boldsymbol{r}_m\})\log(r_{jk}) + H_{\ell m}(\{\boldsymbol{r}_m\})\,, \tag{2.38}$$

where $H_{\ell m}^{jk}(\{\boldsymbol{r}_m\})$ and $H_{\ell m}(\{\boldsymbol{r}_m\})$ are polynomials of degree $2n$. The latter is fully symmetric in the coordinates. The former is symmetric in r_j, r_k and separately in all the other $\{r_m\}_{m\neq i,j}$. It should be noted that (2.38) is merely an ansatz which is justified a posteriori.

Substituting Eq. (2.38) into Eq. (2.33) and collecting terms of the same type yields three equations:

$$\sum_i \nabla_i^2 H_{\ell m}^{jk} = \nabla_j \cdot \nabla_k E_{2n,\ell m}\,, \tag{2.39}$$

$$[1 + \boldsymbol{r}_{jk}\cdot(\boldsymbol{\nabla}_j - \boldsymbol{\nabla}_k)]H_{\ell m}^{jk} + \frac{r_{jk}^{\alpha} r_{jk}^{\beta} \nabla_j^{\alpha}\nabla_k^{\beta}}{4} E_{2n,\ell m} = -\frac{r_{jk}^2 K_{\ell m}^{jk}}{2}\,, \tag{2.40}$$

$$\sum_i \nabla_i^2 H_{\ell m} = \sum_{j\neq k} K_{\ell m}^{jk}\,. \tag{2.41}$$

Here $K_{\ell m}^{jk}$ are polynomials of degree $2n-2$ which are separately symmetric in the j,k coordinates and in all the other coordinates except j,k. In Ref. [21] it was proven that for $\ell = 0$ these equations possess a unique solution. The proof follows through unchanged for any $\ell \neq 0$, and we thus proceed to find the solution.

By symmetry we can specialize the discussion to a particular choice of coordinates, say $j=1$, $k=2$. In light of Eq. (2.40) we see that $H^{12}_{\ell m}$ must have at least a quadratic contribution in r_{12}. This guarantees that (2.38) is nonsingular in the limit $r_{12} \to 0$. The only part of $H^{12}_{\ell m}$ that will contribute to structure functions must contain $\boldsymbol{r}_3 \dots \boldsymbol{r}_{2n}$ at least once. Since $H^{12}_{\ell m}$ has to be a polynomial of degree $2n$ in the coordinates, it must be of the form

$$H^{12}_{\ell m} = r^{\alpha_1}_{12} r^{\alpha_2}_{12} r^{\alpha_3}_{3} \dots r^{\alpha_{2n}}_{2n} C^{\alpha_1\alpha_2\dots\alpha_{2n}}_{\ell m} + [\dots]_{1,2} , \tag{2.42}$$

where $C^{\alpha_1\alpha_2\dots\alpha_{2n}}_{\ell m}$ is some constant tensor and $[\dots]_{1,2}$ contains terms with higher powers of r_{12} and therefore does not contain some of the other coordinates $r_3 \dots r_{2n}$. Obviously, such terms are unimportant for the structure functions. Substituting (2.42) into (2.40) we get

$$5 r^{\alpha_1}_{12} r^{\alpha_2}_{12} r^{\alpha_3}_{3} \dots r^{\alpha_{2n}}_{2n} C^{\alpha_1\alpha_2\dots\alpha_{2n}}_{\ell m} = -\tfrac{1}{4} r^{\alpha_1}_{12} r^{\alpha_2}_{12} r^{\alpha_3}_{3} \dots r^{\alpha_{2n}}_{2n} B^{\alpha_1\dots\alpha_{2n}}_{2n,\ell m} - \tfrac{1}{2} r^{\alpha_1}_{12} r^{\alpha_2}_{12} \delta^{\alpha_1\alpha_2} K^{1,2}_{\ell m} + [\dots]_{1,2} . \tag{2.43}$$

In order to find the tensor $\boldsymbol{C}_{\ell m}$ we need to examine all the terms in the equation that contain $r^{\alpha_1}_{12} r^{\alpha_2}_{12} r^{\alpha_3}_{3} \dots r^{\alpha_{2n}}_{2n}$. One of these is hidden in $K^{1,2}_{\ell m}$. As a function, $K^{1,2}_{\ell m}$ is completely symmetric in $\boldsymbol{r}_3 \dots \boldsymbol{r}_{2n}$ and therefore the part that contains the wanted contribution must be proportional to $r^{\alpha_1}_{12} r^{\alpha_2}_{12} r^{\alpha_3}_{3} \dots r^{\alpha_{2n}}_{2n} \delta^{\alpha_1\alpha_2} B^{\alpha_3\dots\alpha_{2n}}_{2n-2,\ell m}$. It follows that

$$C^{\alpha_1\alpha_2\dots\alpha_{2n}}_{\ell m} = -\tfrac{1}{20} B^{\alpha_1\alpha_2\dots\alpha_{2n}}_{2n,\ell m} + b\delta^{\alpha_1\alpha_2} B^{\alpha_3\alpha_4\dots\alpha_{2n}}_{2n-2,\ell m} , \tag{2.44}$$

where b is some unknown factor originating from $K^{1,2}_{\ell m}$. To find the unknown b we use Eq. (2.39), from which we get:

$$4\delta^{\alpha_1\alpha_2} r^{\alpha_3}_{3} \dots r^{\alpha_{2n}}_{2n} C^{\alpha_1\dots\alpha_{2n}}_{\ell m} = \delta^{\alpha_1\alpha_2} r^{\alpha_3} \dots r^{\alpha_{2n}} B^{\alpha_1\dots\alpha_{2n}}_{2n,\ell m} + [\dots]_{1,2} , \tag{2.45}$$

which implies

$$4\delta^{\alpha_1\alpha_2} C^{\alpha_1\dots\alpha_{2n}}_{\ell m} = \delta^{\alpha_1\alpha_2} B^{\alpha_1\dots\alpha_{2n}}_{2n,\ell m} . \tag{2.46}$$

Recalling identity (A.2) we obtain

$$b = \tfrac{1}{10} z_{2n,\ell} \tag{2.47}$$

and finally,

$$H^{12}_{\ell m} = r^{\alpha_1}_{12} r^{\alpha_2}_{12} r^{\alpha_3}_{3} \dots r^{\alpha_{2n}}_{2n} \left[-\tfrac{1}{20} B^{\alpha_1\alpha_2\dots\alpha_{2n}}_{2n,\ell m} + \tfrac{1}{10} z_{2n,\ell} \delta^{\alpha_1\alpha_2} B^{\alpha_3\alpha_4\dots\alpha_{2n}}_{2n-2,\ell m} \right] . \tag{2.48}$$

In the next subsection we compute from this result the scaling exponents in all the sectors of the SO(3) symmetry group.

2.4. The scaling exponents of the structure functions

We now wish to show that the solution for the zero modes of the correlation functions F_{2n} result in homogeneous structure functions $\mathcal{S}_{2n}$. In every sector (ℓ, m) we compute the scaling exponents, and show that they are independent of m. Accordingly the scaling exponents are denoted by $\zeta_{2n}^{(\ell)}$, and we compute them to first order in ξ.

Using (2.35), (2.36) and (2.48), the structure function is given by

$$\mathcal{S}_{2n,\ell m}(\boldsymbol{r}_1,\bar{\boldsymbol{r}}_1;\ldots;\boldsymbol{r}_{2n},\bar{\boldsymbol{r}}_{2n}) = \Delta_1^{\alpha_1}\ldots\Delta_{2n}^{\alpha_{2n}}B_{2n\ell m}^{\alpha_1\ldots\alpha_{2n}} + \xi\sum_{i\neq j}\overbrace{\Delta_1^{\alpha_1}\ldots\Delta_{2n}^{\alpha_{2n}}}^{\text{no } i,j} f^{\alpha_i\alpha_j}(\boldsymbol{r}_i,\bar{\boldsymbol{r}}_i,\boldsymbol{r}_j,\bar{\boldsymbol{r}}_j)$$
$$\times\left[-\tfrac{1}{20}B_{2n,\ell m}^{\alpha_1\ldots\alpha_{2n}} + \tfrac{1}{10}z_{2n,\ell}\delta^{\alpha_i\alpha_i}\,B_{2n-2,\ell m}^{\overbrace{\alpha_1\ldots\alpha_{2n}}^{\text{no } i,j}}\right], \tag{2.49}$$

where $\Delta_i^{\alpha_i} \equiv r_i^{\alpha_i} - \bar{r}_i^{\alpha_i}$, and the function f is defined as

$$f^{\alpha_i\alpha_j}(\boldsymbol{r}_i,\bar{\boldsymbol{r}}_i,\boldsymbol{r}_j,\bar{\boldsymbol{r}}_j) \equiv (r_i - r_j)^{\alpha_i}(r_i - r_j)^{\alpha_j}\ln|\boldsymbol{r}_i - \boldsymbol{r}_j|$$
$$+(\bar{r}_i - \bar{r}_j)^{\alpha_i}(\bar{r}_i - \bar{r}_j)^{\alpha_j}\ln|\bar{\boldsymbol{r}}_i - \bar{\boldsymbol{r}}_j| \tag{2.50}$$

$$f^{\alpha_i\alpha_j}(\boldsymbol{r}_i,\bar{\boldsymbol{r}}_i,\boldsymbol{r}_j,\bar{\boldsymbol{r}}_j) \equiv -(r_i - \bar{r}_j)^{\alpha_i}(r_i - \bar{r}_j)^{\alpha_j}\ln|\boldsymbol{r}_i - \bar{\boldsymbol{r}}_j|$$
$$-(\bar{r}_i - r_j)^{\alpha_i}(\bar{r}_i - r_j)^{\alpha_j}\ln|\bar{\boldsymbol{r}}_i - \boldsymbol{r}_j|\,. \tag{2.51}$$

The scaling exponent of $\mathcal{S}_{2n,\ell m}$ can be found by multiplying all its coordinates by μ. A direct calculation yields:

$$\mathcal{S}_{2n,\ell m}(\mu\boldsymbol{r}_1,\mu\bar{\boldsymbol{r}}_1;\ldots) = \mu^{2n}\mathcal{S}_{2n,\ell m}(\boldsymbol{r}_1,\bar{\boldsymbol{r}}_1;\ldots) - 2\xi\mu^{2n}\ln\mu\sum_{i\neq j}\overbrace{\Delta_1^{\alpha_1}\ldots\Delta_{2n}^{\alpha_{2n}}}^{\text{no } i,j}\Delta_i^{\alpha_i}\Delta_j^{\alpha_j}$$
$$\times\left[-\tfrac{1}{20}B_{2n,\ell m}^{\alpha_1\ldots\alpha_{2n}} + \tfrac{1}{10}z_{2n,\ell}\delta^{\alpha_i\alpha_j}\,B_{2n-2,\ell m}^{\overbrace{\alpha_1\ldots\alpha_{2n}}^{\text{no } i,j}}\right] + O(\xi^2),$$
$$= \mu^{2n}\mathcal{S}_{2n,\ell m}(\boldsymbol{r}_1,\bar{\boldsymbol{r}}_1;\ldots) - 2\xi\mu^{2n}\ln\mu\Delta_1^{\alpha_1}\ldots\Delta_{2n}^{\alpha_{2n}}$$
$$\times\sum_{i\neq j}\left[-\tfrac{1}{20}B_{2n,\ell m}^{\alpha_1\ldots\alpha_{2n}} + \tfrac{1}{10}z_{2n,\ell}\delta^{\alpha_i\alpha_j}\,B_{2n-2,\ell m}^{\overbrace{\alpha_1\ldots\alpha_{2n}}^{\text{no } i,j}}\right] + O(\xi^2)\,.$$

Using (A.4), we find that

$$\sum_{i\neq j}\left[-\tfrac{1}{20}B_{2n,\ell m}^{\alpha_1\ldots\alpha_{2n}} + \tfrac{1}{10}z_{2n,\ell}\delta^{\alpha_i\alpha_j}\,B_{2n-2,\ell m}^{\overbrace{\alpha_1\ldots\alpha_{2n}}^{\text{no } i,j}}\right] = \left[-2n(2n-1)\tfrac{1}{20} + \tfrac{1}{10}z_{2n,\ell}\right]B_{2n,\ell m}^{\alpha_1\ldots\alpha_{2n}} \tag{2.52}$$

and therefore, we finally obtain:

$$\begin{aligned}&\mathcal{S}_{2n}(\mu \boldsymbol{r}_1, \mu \bar{\boldsymbol{r}}_1; \ldots)\\ &\quad = \mu^{2n}\{1 - 2\xi[-2n(2n-1)\tfrac{1}{20} + \tfrac{1}{10} z_{2n,\ell}] \ln \mu\} \mathcal{S}_{2n}(\boldsymbol{r}_1, \bar{\boldsymbol{r}}_1; \ldots) + O(\xi^2)\\ &\quad = \mu^{\zeta_{2n}^{(l)}} \mathcal{S}_{2n}(\boldsymbol{r}_1, \bar{\boldsymbol{r}}_1; \ldots) + O(\xi^2)\,. \end{aligned} \tag{2.53}$$

The result of the scaling exponent is now evident

$$\zeta_{2n}^{(\ell)} = 2n - \frac{\xi}{10}[2n(2n+3) - 2\ell(\ell+1)] + O(\xi^2)\,. \tag{2.54}$$

For $\ell = 0$ this result coincides with [21]. This is the final result of this calculation.

3. Anisotropy and anomalous scaling in the turbulent advection of passive vectors

In the case of a magnetic field advected by a Gaussian, space homogeneous, δ-correlated velocity field with nontrivial spatial scaling we can present an exact (non-perturbative) solution of the full spectrum of anomalous scaling exponents of all the anisotropic contributions to the covariance of the magnetic field. We can thus offer a precise picture of the rate of isotropization upon diminishing scales, assess the importance of anisotropy for "inertial range" scaling, etc.

The equation of motion of a magnetic field $\boldsymbol{B}(\boldsymbol{r}, t)$ reads

$$\partial_t \boldsymbol{B}(\boldsymbol{r}, t) + \boldsymbol{u}(\boldsymbol{r}, t) \cdot \boldsymbol{\nabla} \boldsymbol{B}(\boldsymbol{r}, t) = \boldsymbol{B}(\boldsymbol{r}, t) \cdot \boldsymbol{\nabla} \boldsymbol{u}(\boldsymbol{r}, t) + \kappa \nabla^2 \boldsymbol{B}(\boldsymbol{r}, t) + \boldsymbol{f}(\boldsymbol{r}, t)\,, \tag{3.1}$$

where $\boldsymbol{u}$ is the same advecting velocity field as in Section 2, $\boldsymbol{f}$ is the external forcing, and κ is the magnetic diffusivity. As before, the correlation function of the forcing has compact support in $\boldsymbol{k}$-space in an interval $0 \leqslant k \leqslant 1/L$, where L is the outer scale of the forcing $\boldsymbol{f}$. We denote

$$\langle f^\alpha(\boldsymbol{R}, t) f^\beta(0, t') \rangle_{\boldsymbol{f}} \equiv F^{\alpha\beta}(\boldsymbol{R}) \delta(t - t')\,. \tag{3.2}$$

We are interested in the properties of the covariance of $\boldsymbol{B}$, $C^{\alpha\beta}(\boldsymbol{R}, t)$,

$$C^{\alpha\beta}(\boldsymbol{R}, t) \equiv \langle B^\alpha(\boldsymbol{R}, t) B^\beta(0, t) \rangle_{\boldsymbol{u}, \boldsymbol{f}} \tag{3.3}$$

and eventually in the stationary quantity $C^{\alpha\beta}(\boldsymbol{R})$ which is obtained in the stationary state if the forcing is balanced by dissipation. There is a possibility of a dynamo effect in such equations, but in Ref. [14] we have shown that there is no dynamo effect in the anisotropic sectors of the covariance. We will therefore, proceed here to describe the calculations without further reference to dynamos.

To proceed, we consider the equation of motion of the covariance in the stationary case [10,11]:

$$\begin{aligned} 0 = \partial_t C^{\alpha\beta} &= h^{\mu\nu} \partial_\mu \partial_\nu C^{\alpha\beta} - [(\partial_\nu h^{\mu\beta}) \partial_\mu C^{\alpha\nu} + (\partial_\nu h^{\alpha\mu}) \partial_\mu C^{\nu\beta}]\\ &\quad + (\partial_\mu \partial_\nu h^{\alpha\beta}) C^{\mu\nu} + 2\kappa \nabla^2 C^{\alpha\beta} + F^{\alpha\beta} \equiv \hat{T}^{\alpha\beta}_{\sigma\rho} C^{\sigma\rho} + F^{\alpha\beta}\,, \end{aligned} \tag{3.4}$$

$$\partial_\alpha C^{\alpha\beta} = 0\,, \tag{3.5}$$

where the last equation follows from the solenoidal condition for the magnetic field.

It is advantageous to decompose the covariance $C^{\alpha\beta}$ in terms of basis functions that block-diagonalize the angular part of the differential operator $\hat{T}^{\alpha\beta}_{\sigma\rho}$. These basis functions are implied by the symmetries of $\hat{T}^{\alpha\beta}_{\sigma\rho}$. Since this operator contains only isotropic differential operators and contractions with either $\delta^{\alpha\beta}$ or $R^\alpha R^\beta$, it is invariant to all rotations [1]. Accordingly, as in all the examples above, the natural basis functions should belong to irreducible representation of the SO(3) symmetry group, and can be indexed by pairs of indices ℓ, m. The operator $\hat{T}^{\alpha\beta}_{\sigma\rho}$ leaves the ℓ, m sectors invariant. In addition, $\hat{\boldsymbol{T}}$ is invariant to the parity transformation $\boldsymbol{R} \to -\boldsymbol{R}$, and to the index permutation $(\alpha, \mu) \Leftrightarrow (\beta, \nu)$. Accordingly, $\hat{\boldsymbol{T}}$ can be further block-diagonalized into blocks with definite parity and symmetry under permutations.

In light of these considerations we seek solutions of the form

$$C^{\alpha\beta}(\boldsymbol{R}, t) = \sum_{q,\ell,m} a_{q\ell m}(|\boldsymbol{R}|, t)\, B^{\alpha\beta}_{q\ell m}(\hat{\boldsymbol{R}}) , \tag{3.6}$$

where $\hat{\boldsymbol{R}} \equiv \boldsymbol{R}/R$, and $B^{\alpha\beta}_{q\ell m}(\hat{\boldsymbol{R}})$ are tensor functions on the unit sphere, which belong to the sector (ℓ, m) of the SO(3) symmetry group. The index q enumerates different tensor functions belonging to the same sector. While for scalar functions on the sphere there exists only one spherical harmonic $Y_{\ell m}$ in each sector, for the second rank tensor functions on the sphere there exist nine different tensors [1]. The additional symmetries under parity and index permutation group them into four subgroups with four, two, two and one tensors, respectively. With $\Phi_{\ell m}(\boldsymbol{R}) \equiv R^\ell Y_{\ell m}(\hat{\boldsymbol{R}})$, in the notation of [1], the 4-group (denoted below as subset I) is

$$B^{\alpha\beta}_{9\ell m}(\hat{\boldsymbol{R}}) \equiv R^{-\ell-2} R^\alpha R^\beta \Phi_{\ell m}(\boldsymbol{R}) ,$$

$$B^{\alpha\beta}_{7\ell m}(\hat{\boldsymbol{R}}) \equiv R^{-\ell}(R^\alpha \partial^\beta + R^\beta \partial^\alpha)\Phi_{\ell m}(\boldsymbol{R}) ,$$

$$B^{\alpha\beta}_{1\ell m}(\hat{\boldsymbol{R}}) \equiv R^{-\ell} \delta^{\alpha\beta} \Phi_{\ell m}(\boldsymbol{R}) ,$$

$$B^{\alpha\beta}_{5\ell m}(\hat{\boldsymbol{R}}) \equiv R^{-\ell+2} \partial^\alpha \partial^\beta \Phi_{jm}(\boldsymbol{R}) . \tag{3.7}$$

These are all symmetric in α, β and have a parity of $(-1)^j$. The 2-groups are denoted, respectively, as subsets II and III:

$$B^{\alpha\beta}_{8\ell m}(\hat{\boldsymbol{R}}) \equiv R^{-\ell-1}[R^\alpha \varepsilon^{\beta\mu\nu} R_\mu \partial_\nu + R^\beta \varepsilon^{\alpha\mu\nu} R_\mu \partial_\nu]\Phi_{\ell m}(\boldsymbol{R}) ,$$

$$B^{\alpha\beta}_{6\ell m}(\hat{\boldsymbol{R}}) \equiv R^{-\ell+1}[\varepsilon^{\beta\mu\nu} R_\mu \partial_\nu \partial^\alpha + \varepsilon^{\alpha\mu\nu} R_\mu \partial_\nu \partial^\beta]\Phi_{\ell m}(\boldsymbol{R}) . \tag{3.8}$$

$$B^{\alpha\beta}_{4\ell m}(\hat{\boldsymbol{R}}) \equiv R^{-\ell-1} \varepsilon^{\alpha\beta\mu} R_\mu \Phi_{\ell m}(\boldsymbol{R}) ,$$

$$B^{\alpha\beta}_{2\ell m}(\hat{\boldsymbol{R}}) \equiv R^{-\ell+1} \varepsilon^{\alpha\beta\mu} \partial_\mu \Phi_{\ell m}(\boldsymbol{R}) . \tag{3.9}$$

The first couple is symmetric to α, β exchange and has parity $(-1)^{\ell+1}$. The second has the same parity but is antisymmetric to α, β exchange. The remaining basis function is $B^{\alpha\beta}_{3\ell m}(\hat{\boldsymbol{R}}) \equiv R^{-\ell}(R^\alpha \partial^\beta - R^\beta \partial^\alpha)\Phi_{\ell m}(\boldsymbol{R})$ which is antisymmetric to α, β exchange, with parity $(-1)^\ell$. This will be denoted as subset IV. In Ref. [1] it was proven that this basis is complete and indeed transforms under rotations as required for a ℓ, m sector.

It should be noted that not all subsets contribute for every value of ℓ. Space homogeneity implies the obvious symmetry of the covariance:

$$C^{\alpha\beta}(\boldsymbol{R}, t) = C^{\beta\alpha}(-\boldsymbol{R}, t) . \tag{3.10}$$

Therefore, representations symmetric to $\alpha \Leftrightarrow \beta$ exchange must also have even parity, while antisymmetric representations must have odd parity. Accordingly, even ℓ's are associated with subsets I and III, and odd ℓ's are associated with subset II. In addition, it was shown in Ref. [14] that subset IV cannot contribute to this theory due to the solenoidal constraint.

The calculation of the stationary solutions becomes rather immediate once we know the functional form of the operator $\hat{\boldsymbol{T}}$ on the basis of the angular tensors $\boldsymbol{B}_{q\ell m}(\hat{\boldsymbol{R}})$. In this representation, $\hat{\boldsymbol{T}}$ is a linear differential operator, acting on the *coefficients* $a_{q\ell m}(|\boldsymbol{R}|)$. The symmetries described above ensure that $\hat{\boldsymbol{T}}$ will only mix $a_{q\ell m}(|\boldsymbol{R}|)$ with the same ℓ, m, that belong to the same subset. $\hat{\boldsymbol{T}}$ will therefore be composed of blocks of sizes 4×4 and 2×2. In Ref. [14] we give the full functional form of these blocks. Here we shall use them symbolically and quote the final results. To demonstrate this point, consider the four-dimensional block of $\hat{\boldsymbol{T}}$, created by the four basis tensors $\boldsymbol{B}_{q\ell m}$ of subset I. To simplify the notation, we denote the coefficients of these angular tensors in (3.6), by the four functions $a(R), b(R), c(R), d(R)$:

$$C^{\alpha\beta}(\boldsymbol{R}) \equiv a(R)B^{\alpha\beta}_{9,\ell m}(\hat{\boldsymbol{R}}) + b(R)B^{\alpha\beta}_{7,\ell m}(\hat{\boldsymbol{R}}) + c(R)B^{\alpha\beta}_{1,\ell m}(\hat{\boldsymbol{R}}) + d(R)B^{\alpha\beta}_{5,\ell m}(\hat{\boldsymbol{R}}) + \dots , \tag{3.11}$$

where $(\dots)$ stand for terms with other (ℓ, m) and other symmetries with the same (ℓ, m). Plugging this expansion into the equation of motion (3.4), we get a set of four ODEs for the coefficients $a(R), b(R), c(R), d(R)$:

$$\boldsymbol{T}_1 \begin{pmatrix} a'' \\ b'' \\ c'' \\ d'' \end{pmatrix} + \boldsymbol{T}_2 \begin{pmatrix} a' \\ b' \\ c' \\ d' \end{pmatrix} + \boldsymbol{T}_3 \begin{pmatrix} a \\ b \\ c \\ d \end{pmatrix} = 0 . \tag{3.12}$$

$\boldsymbol{T}_1, \boldsymbol{T}_2, \boldsymbol{T}_3$ are 4×4 matrices given explicitly in Ref. [14] which depend on R, ℓ, ξ, D, κ. Adding the forcing will just result in the addition of a possible inhomogeneous term to this equation. This term is irrelevant to the calculation of the zero-modes of Eq. (3.4).

Deep in the inertial range we look for scale-invariant solutions, obtained as zero-modes of Eq. (3.4). Indeed, when $\xi > 0$ and well within the inertial range we can take the magnetic dissipation to zero, and as a result, the homogeneous part of Eq. (3.4) (without $F^{\alpha\beta}$) will be scale-invariant, leading to scale-invariant solutions. We will need to match these zero modes to the appropriate zero modes computed in the dissipative range at the end. This will necessitate the discussion of zero modes when $\xi = 0$, and see below.

Let us first consider the case where $\xi > 0$. According to (3.12), well within the inertial range, these functions obey

$$\boldsymbol{T}_1(\kappa=0)\begin{pmatrix} a'' \\ b'' \\ c'' \\ d'' \end{pmatrix} + \boldsymbol{T}_2(\kappa=0)\begin{pmatrix} a' \\ b' \\ c' \\ d' \end{pmatrix} + \boldsymbol{T}_3(\kappa=0)\begin{pmatrix} a \\ b \\ c \\ d \end{pmatrix} = 0\,. \tag{3.13}$$

Using the explicit functional form of $T_1(\kappa=0), T_2(\kappa=0), T_3(\kappa=0)$ (given in Ref. [14]), we remove an overall factor of DR^{ζ} from (3.13), and obtain the simple scale-invariant equation:

$$2\begin{pmatrix} a'' \\ b'' \\ c'' \\ d'' \end{pmatrix} + \frac{2}{R}\begin{pmatrix} a' \\ b' \\ c' \\ d' \end{pmatrix} + \frac{\boldsymbol{Q}(\ell,\zeta)}{R^2}\begin{pmatrix} a \\ b \\ c \\ d \end{pmatrix} = 0\,. \tag{3.14}$$

$\boldsymbol{Q}(\ell,\zeta)$ is a 4×4 matrix given in Ref. [14].

Due to the scale invariance of this equation, we look for scale-invariant solutions in the form:

$$a(R) = aR^{\zeta}, \quad b(R) = bR^{\zeta}, \quad c(R) = cR^{\zeta}, \quad d(R) = dR^{\zeta}\,. \tag{3.15}$$

Where a,b,c,d are complex constants. Substituting (3.15) into (3.14) results in a set of four linear homogeneous equations for the unknowns a,b,c,d:

$$[2\zeta(\zeta-1)\mathbb{1} + 2\zeta\mathbb{1} + \boldsymbol{Q}(\ell,\xi)]\begin{pmatrix} a \\ b \\ c \\ d \end{pmatrix} = 0\,. \tag{3.16}$$

The last equation admits non-trivial solutions only when

$$\det[2\zeta(\zeta-1)\mathbb{1} + 2\zeta\mathbb{1} + \boldsymbol{Q}(\ell,\xi)] = 0\,. \tag{3.17}$$

This solvability condition allows us to express ζ as a function of ℓ and ξ. Using MATHEMATICA we find eight possible values of ζ, out of which, only four are in agreement with the solenoidal condition:

$$\begin{aligned} &\zeta_i^{(\ell)} = -\tfrac{1}{2}\xi - \tfrac{3}{2} \pm \tfrac{1}{2}\sqrt{H(\xi,\ell) \pm 2\sqrt{K(\xi,\ell)}}\,, \\ &K(\xi,\ell) \equiv \xi^4 - 2\xi^3 + 2\xi^3\ell + 2\xi^3\ell^2 - 4\xi^2\ell - 3\xi^2 - 4\xi^2\ell^2 \\ &\qquad\qquad -8\xi\ell^2 - 8\xi\ell + 4\xi + 16\ell + 16\ell^2 + 4\,, \\ &H(\xi,\ell) \equiv -\xi^2 - 8\xi + 2\xi\ell^2 + 2\xi\ell + 4\ell^2 + 4\ell + 5\,. \end{aligned} \tag{3.18}$$

Not all of these solutions are physically acceptable because not all of them can be matched to the zero mode solutions in the dissipative regime. To see why this is so, consider the zero-mode equation for $\xi = 0$:

$$(2\kappa + 2D)\nabla^2\boldsymbol{C} = 0\,. \tag{3.19}$$

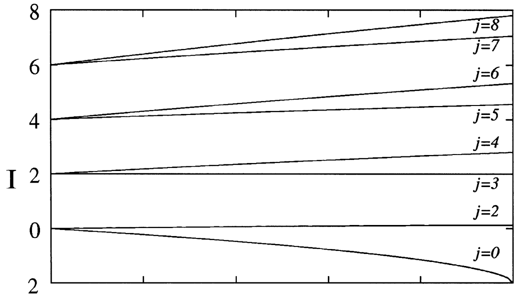

Fig. 1. The leading exponents of the symmetric parts of the zero modes of the magnetic covariance.

The main difference between the $\xi = 0$ case and the $\xi > 0$ case is that in the former the same scale-invariant equation holds *both* for the inertial range and the dissipative range. As a result, for $\xi = 0$, the zero modes scale with the same exponents in the two regimes. These exponents are given simply by (3.18) with $\xi = 0$, because for $\xi = 0$ the zero modes equation with $\kappa = 0$ is the same Laplace equation as (3.19) up to the overall factor $D/(D+\kappa)$ which does not change the exponent. Since now our solutions should be valid for the dissipative regime as well as for the inertial regime, the two solutions with negative exponents in (3.18) are ruled out, for they will give a nonphysical divergence as $R \to 0$. Assuming now that the solutions (including the exponents) are continuous in ξ, (and not necessarily analytic!), we find that also for finite ξ only the positive exponents appear in the inertial range (an exception to that is the $\ell = 0$, to be discussed below).

Finally, there exist two branches of solutions corresponding to the $(-)$ and $(+)$ in the square root.

$$\zeta_{I\pm}^{(\ell)} = -\frac{3}{2} - \frac{1}{2}\xi + \frac{1}{2}\sqrt{H(\xi,\ell) \pm 2\sqrt{K(\xi,\ell)}} \quad \text{subset I} . \tag{3.20}$$

These exponents are in agreement with [10,11,6]. Note that for $\ell = 0$, only $\zeta_{I+}^{(0)}$ exists since the other exponent is not admissible, being negative for $\xi \to 0$, and therefore, excluded by continuity. $\zeta_{I+}^{(0)}$ however, becomes negative as ξ increases (see Fig. 1). For $\ell \geqslant 2$ both solutions are admissible, and the leading one is $\zeta_{I-}^{(0)}$, which is smaller.

Let us find the behavior of the zero modes in the dissipative regime for $\xi > 0$. Here the dissipation terms become dominant and we can neglect all other terms in $\hat{\boldsymbol{T}}$. The zero mode equation in this regime becomes $2\kappa\nabla^2 C^{\alpha\beta} = 0$, which is again, up to an overall factor, identical to the zero mode equation with $\kappa = 0$, $\xi = 0$. The solutions in this region are once again scale invariant with scaling exponents $\zeta_{I\pm}^{(\ell)}|_{\xi=0} = \ell, \ell - 2$. As expected, the correlation function $C^{\alpha\beta}(\boldsymbol{R})$ becomes smooth in the dissipative regime.

In addition to subset I, one needs to compute the exponents corresponding to subsets II and III. The computation in the other two blocks follows the same lines. Since these are 2×2 they furnish two solutions for the exponents, one of which is negative. We

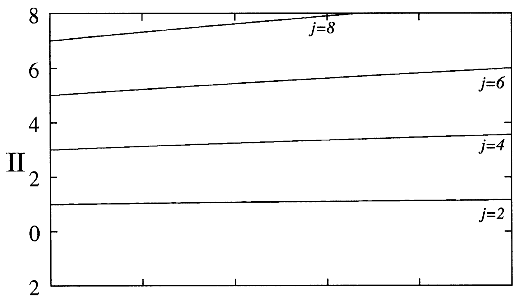

Fig. 2. The leading exponents of the antisymmetric parts of the zero modes of the magnetic covariance.

Table 1
The leading exponents in the various sectors

	Symmetric	AntiSymmetric
$j = 0$	ζ_{I+}	–
Even $j > 0$	ζ_{I-}	ζ_{III}
Odd $j > 1$	ζ_{II}	–

end up finding

$$\zeta_{II}^{(\ell)} = -\frac{3}{2} - \frac{1}{2}\xi + \frac{1}{2}\sqrt{1 - 10\xi + \xi^2 + 2\ell^2\xi + 2\ell\xi + 4\ell + 4\ell^2} \quad \text{subset II}\,, \tag{3.21}$$

$$\zeta_{III}^{(\ell)} = -\frac{3}{2} - \frac{1}{2}\xi + \frac{1}{2}\sqrt{\xi^2 + 2\xi + 1 + 4\ell^2 + 2\ell^2\xi + 4\ell + 2\xi\ell} \quad \text{subset III}\,. \tag{3.22}$$

For $\ell = 0$ there is no contribution from this subset, as the exponent is negative. The dependence of the admissible leading exponents on ξ is displayed in Figs. 1 and 2. In Table 1 we summarize the leading exponents in each sector.

After matching the zero modes to the dissipative range, one has to guarantee matching at the outer scale L. The condition to be fulfilled is that the sum of the zero-modes with the inhomogeneous solutions (whose exponents are $2 - \xi$) must give $\boldsymbol{C}(\boldsymbol{R}) \to 0$ as $|\boldsymbol{R}| \to L$. Obviously, this means that the forcing must have a projection on any sector $\boldsymbol{B}_{q\ell m}$ for which $a_{q\ell m}$ is nonzero.

4. Navier–Stokes turbulence

We cannot describe in this short review all the work that has been done by our group on anisotropic hydrodynamic turbulence, and the reader is referred to Refs. [1–4] for further information. Yet, we cannot close this review without the mention of this subject, since most of the available data analysis and theoretical thinking about the universal statistics of the small-scale structure of turbulence assume the existence of an idealized model of homogeneous and isotropic flow. In fact most realistic flows are neither homogeneous nor isotropic. Accordingly, one can analyze the data pertaining to such flows in two ways. The traditional one has been to disregard the inhomogeneity and anisotropy, and proceed with the data analysis assuming that the results pertain to the homogeneous and isotropic flow. The second, which is advocated all along this review, is to take the anisotropy explicitly into account, to carefully decompose the relevant statistical objects into their isotropic and anisotropic contributions, and assess the degree of universality of each component separately.

As a demonstration of the utility of our approach we will review briefly our analysis of direct numerical simulations of a channel flow with $\mathrm{Re}_\lambda \approx 70$ [22–24]. This flow has a mean shear, and the analysis revealed the importance of contributions belonging to the anisotropic sectors. After proper decomposition in the SO(3) sectors we found that even for this relatively low value of Re, in each sector one finds respectable scaling behaviour that is masked altogether by a sum of scaling contributions without the SO(3) decomposition. The exponents found at this low values of the Reynolds number for the $\ell=0$ (isotropic) sector are in excellent agreement with high Re results; these exponents are invariant to the position in the inhomogeneous flow, leading to reinterpretation of recent findings of position dependence as resulting from the intervention of the anisotropic sectors. The latter have nonuniversal weights that depend on the position in the flow. In the anisotropic sectors we find scaling exponents that appear universal and in agreement with our analysis of experimental data taken in the atmospheric boundary layers. We will now briefly describe the method of analysis and later summarize the present knowledge concerning the exponents in the various sectors of the symmetry group.

4.1. Analysis of simulations

We consider here channel flow simulations on a grid of 256 points in the stream-wise direction $\hat{x}$, and (128×128) in the other two directions, $\hat{y}, \hat{z}$. We denote by $\hat{z}$ the direction perpendicular to the walls and by $\hat{y}$ the span-wise direction in planes parallel to the walls. We employ periodic boundary conditions in the span-wise and stream-wise directions and no-slip boundary conditions on the walls. The Reynolds number based on the Taylor scale is $\mathrm{Re}_\lambda \approx 70$ in the center of the channel ($z=64$). The simulation is fully symmetric with respect to the central plane. The flow correctly develops a mean profile in the stream-wise direction which depends only on the distance from the wall, $U_x(z)$. The mean profile shows the three typical regimes: a laminar linear mean profile inside the viscous sublayers, a logarithmic profile for intermediate distances and finally a parabolic mean profile in the core of the channel. For more details on the averaged quantities and on the numerical code the reader is referred to Refs. [22,24].

Previous analysis of the same data-base [22] as well as of other DNS [25] and experimental data [26,27] in anisotropic flows found that the scaling properties of energy spectra, energy co-spectra and of longitudinal structure functions exhibit strong dependence on the local degree of anisotropy. For example, in Ref. [23] the authors studied the longitudinal structure functions at fixed distances from the walls

$$S^{(p)}(R,z) \equiv \langle (v_x(x+R,y,z) - v_x(x,y,z))^p \rangle \,, \tag{4.1}$$

where $\langle \cdots \rangle$ denotes a spatial average on a plane at a fixed height z, $1 < z < 64$. For this set of observables they found that: (i) These structure functions did not exhibit clear scaling behavior as a function of the distance R. Consequently, one needed to resort to extended-self-similarity (ESS]) [28] in order to extract a set of relative scaling exponents $\hat{\zeta}_p \equiv \zeta_p/\zeta_3$; (ii) the relative exponents, $\hat{\zeta}_p$ depended strongly on the height z. Moreover, only at the center of the channel and very close to the walls the error bars on the relative scaling exponents extracted by using ESS were small enough to claim the very existence of scaling behavior in any sense. Similarly, an experimental analysis of a turbulent flow behind a cylinder [26] showed a strong dependence of the relative scaling exponents on the position behind the cylinder for not too big distances from the obstacle, i.e. where anisotropic effects may still be relevant in a wide range of scales. In the following we present an interpretation of the variations in the scaling exponents observed in nonisotropic and nonhomogeneous flows upon changing the position in which the analysis is performed. In particular, we will show that decomposing the statistical objects into their different (j,m) sectors rationalizes the findings, i.e. scaling exponents in given (j,m) sector appear quite independent of the spatial location; only the *amplitudes* of the SO(3) decomposition depend strongly on the spatial location. These findings, if confirmed by other independent measurements, would suggest that the apparent dependence of scaling exponents for longitudinal structure functions on the location in a non-homogeneous flow results from of a superposition of power laws each of which is characterized by its own *universal* scaling exponent. The amplitudes of the various contributions may depend on the local degree of anisotropy and nonhomogeneity.

Our method of analysis is quite simple. We start by a direct measurement of the longitudinal structure functions

$$S_p(\boldsymbol{r}^c, \boldsymbol{R}) = \langle [(\boldsymbol{u}(\boldsymbol{r}^c + \boldsymbol{R}) - \boldsymbol{u}(\boldsymbol{r}^c - \boldsymbol{R})) \cdot \hat{\boldsymbol{R}}]^p \rangle \,. \tag{4.2}$$

Note that the two velocity fields are measured at the extremes of the diameter of a sphere of radius R centered at $\boldsymbol{r}^c$. Due to the inhomogeneity this function depends explicitly on $\boldsymbol{r}^c$. Due to the anisotropy, the function depends on the orientation of the separation vector $2\boldsymbol{R}$ as well as on its magnitude. The average must be taken over different time frames. Typically, we have used 160 time frames for such an average. The time frames are separated by about one eddy turn over time. In each time frame we also improved the statistics by averaging over one fourth of the total number of spatial points in the plane at fixed z, invoking the homogeneity in the span-wise and stream-wise directions, $\hat{x}, \hat{y}$. Thus we have finally about 1×10^6 contributions to each average.

Having computed $S_p(\boldsymbol{r}^c, \boldsymbol{R})$ we decompose it into the irreducible representations of the SO(3) symmetry group according to:

$$S_p(\boldsymbol{r}^c, \boldsymbol{R}) = \sum_{\ell,m} S_{p,\ell,m}(\boldsymbol{r}^c, |\boldsymbol{R}|) Y_{\ell,m}(\hat{\boldsymbol{R}}) . \tag{4.3}$$

We expect that when scaling behavior sets in (presumably at high enough Re) we should find:

$$S_{p,\ell,m}(\boldsymbol{r}^c, |\boldsymbol{R}|) \sim a_{\ell,m}(\boldsymbol{r}^c)|R|^{\zeta_p^{(\ell)}} . \tag{4.4}$$

In other words, we expect [1] the scaling exponent $\zeta_p^{(\ell)}$ to be independent of m, as was shown explicitly for the passive scalar and passive vector examples treated above.

In Fig. 1 we show (i) the log–log plot of the raw structure function (4.2) with $p=4$ measured on the central plane with the vector $\mathbf{R}$ in the streamwise direction, $\mathbf{R} = R\hat{x}$, and (ii) the fully isotropic sector $S_{4,00}(\mathbf{r}^c, |\mathbf{R}|)$ with the average in (4.2) taken on the sphere centered on the central plane $r_z^c = 64$.

It appears that already at this fairly low Reynolds number, the $\ell = 0$ sector shows decent scaling behavior as a function of R. This is in marked contrast with the raw structure function for which no scaling behavior is detectable ($\times$ symbols in Fig. 1). For the raw quantity, the method of "extended-self-similarity" (ESS) [28] is unavoidable if one wants to extract any kind of apparent scaling exponent. In our analysis we found similar results also for higher order structure functions. The scaling behavior is improved dramatically for the components and it can be seen even without ESS.

The second point we would like to stress is the apparent *invariance* of the scaling exponents belonging to the same (j,m) sector with respect to changing the spatial location in the flow. To study this issue quantitatively we resort to ESS, and examine the relative scaling of, say, structure functions of order n with respect to the structure function of order 2 for $n = 3, 4\ldots$. The ESS method is applied in each (ℓ, m) sector separately.

In Fig. 2 we show two typical ESS plots for longitudinal structure functions of order 4 vs. longitudinal structure functions of order 2 both at the center $z=64$ and at $z=32$ in the sector $\ell = 0$. Also, in the inset the quality of the scaling can be appreciated by looking at the *logarithmic local slopes* of $\log(S_{4,00}(\mathbf{r}^c, |R|))$ vs. $\log(S_{2,00}(\mathbf{r}^c, |R|))$ as a function of R for the same two different central positions of the sphere: at the center of the channel ($r_z^c = 64$) and at one quarter of the total channel height ($r_z^c = 32$). The two curves give the same global relative scaling exponent. We compute the scaling exponents by numerical differentiation and fitting; the best fits for the relative scaling exponents in the sector ($\ell=0$) give $\hat{\zeta}_4^{(0)}(z=64) \equiv \zeta_4^{(0)}(z=64)/\zeta_2^{(0)}(z=64) = 1.84 \pm 0.05$ at the center and $\hat{\zeta}_4^{(0)}(z = 32) = 1.82 \pm 0.04$ at $r_z^c = 32$. This result is remarkable and together with the experimental result of Ref. [2] it provides strong evidence for the universality of scaling exponent as defined in distinct (ℓ, m) sectors. We recall that the accepted value of this relative exponent in high-Re experiments is $\zeta_4/\zeta_2 \approx 1.82 \pm 0.02$.

Similarly, but affected from larger error bars, one recovers the same invariance with respect to higher-order moments. For instance, we measure $\hat{\zeta}_6^{(0)}(z=64) \sim \hat{\zeta}_6^{(0)}(z=32) = 2.5 \pm 0.1$. As for relative scaling exponents of higher j sectors, the scaling is less clean and therefore we may only quote qualitative estimates. As an example, for relative scaling exponents of the $(j=2, m=2)$ and $(j=2, m=0)$ sectors we have $\hat{\zeta}_4^{(2,0)}(z=64) = 1.1 \pm 0.1$, $\hat{\zeta}_4^{(2,0)}(z=32) = 1.15 \pm 0.1$, $\hat{\zeta}_4^{(2,2)}(z=64) = 1.3 \pm 0.1$, $\hat{\zeta}_4^{(2,2)}(z=32) = 1. \pm 0.1$.

To underline the quantitative improvement resulting from the application of the SO(3) decomposition we show in Fig. 3 the *logarithmic local slopes* of the raw structure functions $S_4(r_z^c, R\hat{x})$ vs. $S_2(r_z^c, R\hat{x})$ at $r_z^c = 64$ and at $r_z^c = 32$. Also the *logarithmic local slopes* of the projection on the $\ell = 0$ sector at the same two distances from the walls are presented. As is evident, the raw structure function at the center of the channel and the two $j = 0$ projections are in good agreement with the high Reynolds numbers estimate $\zeta(4)/\zeta(2) = 1.82$ while a clearly spurious departure is seen for the raw structure functions at $r_c^z = 32$.

Finally, we discuss briefly the determination of the scaling exponents associated with higher ℓ sectors.

In Fig. 4 we show the log–log plot of $S_{2,\ell,m}(\mathbf{r}^c, |R|)$ vs. $|R|$ for $(\ell = 2, m = 2)$ at the center of the channel, and for $(\ell = 2, m = 2)$ and $(\ell = 2, m = 0)$ at $r_z^c = 32$, superimposed with the straight line with slope $\frac{4}{3}$. The agreement is quite good. Considering the relatively low Reynolds numbers and the fact that the projections on the different sectors depend on the nonuniversal prefactors $a_{\ell,m}$ in decomposition (4.4), we think that together with the experimental result reported in Refs. [2,4] the present finding gives strong support to the view that the scaling exponents in the $\ell = 2$ sector are universal (Figs. 5 and 6).

4.2. Summary of what is known about the anisotropic sectors in hydrodynamic turbulence

For the sake of the interested reader we summarize here what, we believe, is known at present about the scaling exponents in the higher sectors of the symmetry group in hydrodynamic turbulence.

We believe that one can quote, with relative confidence, numerical values of the scaling exponents of the second order correlation function for $j = 0, 1$ and 2. The best current estimates are $\zeta_2^{(0)} \approx 0.69$, $\zeta_2^{(1)} \approx 1.0$, $\zeta_2^{(2)} \approx 1.35$. These values can be understood (disregarding the relatively small intermittency corrections) on the level of dimensional analysis (which predicts $\frac{2}{3}$, 1 and $\frac{4}{3}$, respectively) as has been argued in Ref. [4].

Another point that can be readily stated with confidence is that the effects or the anisotropic contributions increase in importance with the order of the structure function. In numerical simulations in which we can project onto any irreducible representation, we can measure the relative weight of the isotropic $j = 0$ contribution relative to all the

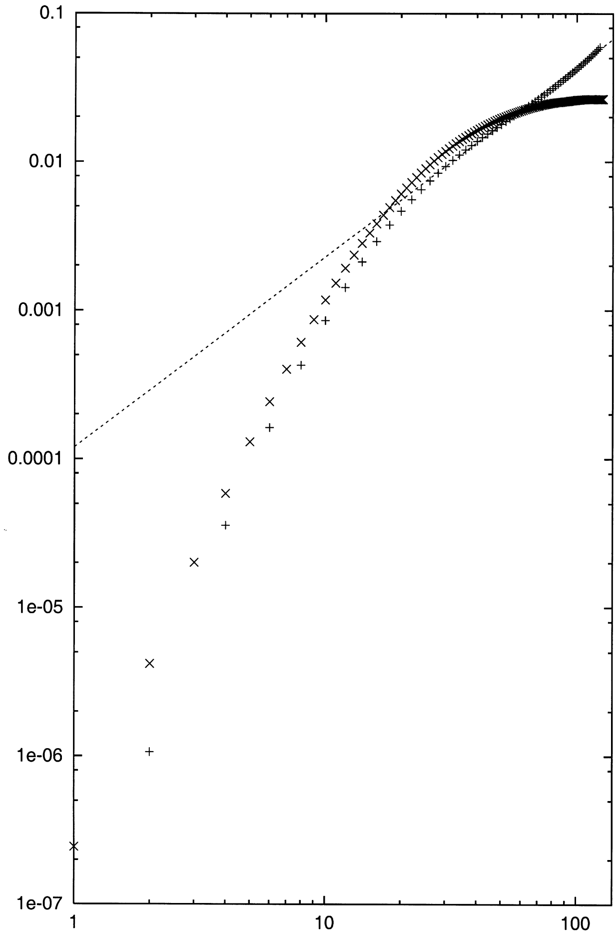

Fig. 3. Log-log plot of the isotropic sector of the fourth-order structure function $S_{4,00}$, vs. R at the center of the channel $r_z^c = 64$ (+). The data represented by (×) correspond to the raw longitudinal structure function, $S_4(r_z^c = 64, R\hat{x})$ averaged over the central plane only. The dashed line corresponds to the intermittent isotropic high Reynolds numbers exponents $\zeta_4^{(0)} = 1.28$.

rest. *This relative weight goes down rapidly with the order of the structure function.* This finding indicates that *for any quantitative determination of ζ_n for high values of n one cannot avoid taking into account the effects of anisotropy.*

5. Summary and discussion

The picture that emerges from all the examples dealt with so far is that, compared to the isotropic sector, all the higher order sectors are characterized by scaling exponents that are larger. In the cases of passive scalar and passive vector, the spectrum is strictly

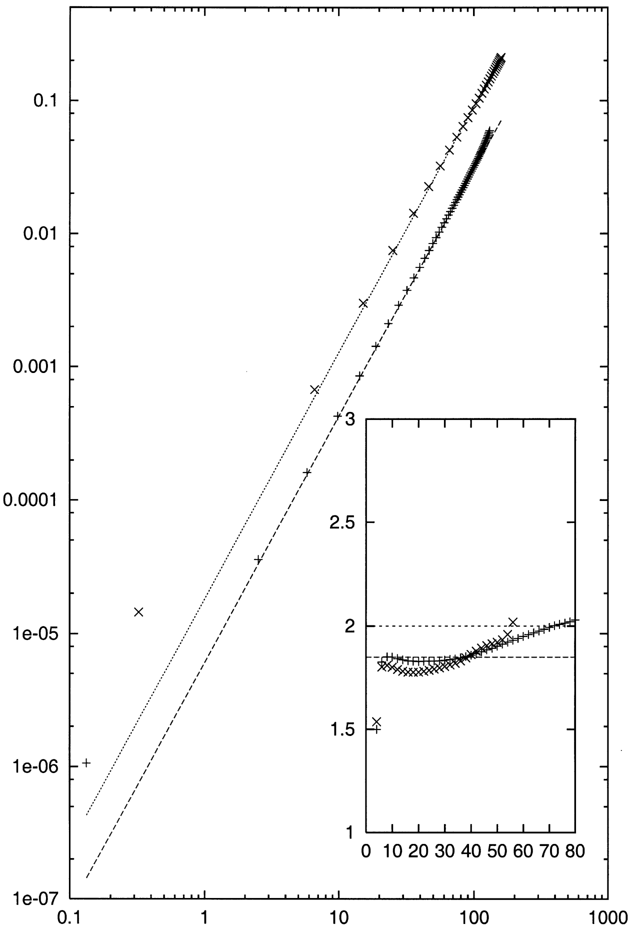

Fig. 4. Isotropic sector: ESS plot of $\log S_{4,00}$ vs. $\log S_{2,00}$ at the center, $r_z^c = 64$, (bottom curve) and at $r_z^c = 31$ (top curve), the straight lines are the best fits with slope 1.82. Inset: local slope of $\log S_{4,00}$, vs. $\log S_{2,00}$ as a function of R, for two different locations in the channel: (+) center of the channel $r_z^c = 64$, (×) one quarter of the total height $r_z^c = 32$. The local slopes are very close. For comparison we have also plotted a horizontal curve corresponding to the accepted anomalous high Reynolds number value, $\zeta_4/\zeta_2 = 1.82$.

increasing for all values of ℓ. In hydrodynamic turbulence this is not known and may not be so, but still the exponents in sectors with $\ell > 0$ are larger than the fundamental exponent in the isotropic sector which for the second-order structure function is about 0.69. If this is so, it may explain the decay of anisotropy at small scales for high Re flows. In the limit Re $\to \infty$ we expect scaling behavior at very small values of R/L with L being the outer scale. At such small scales only the smallest exponent survives, and this is how the alleged universality of the small scales is achieved.

Nevertheless, one needs to understand that the effects of anisotropy on *some* quantities may persist for arbitrarily small scales and arbitrarily high Re. Any quantity that

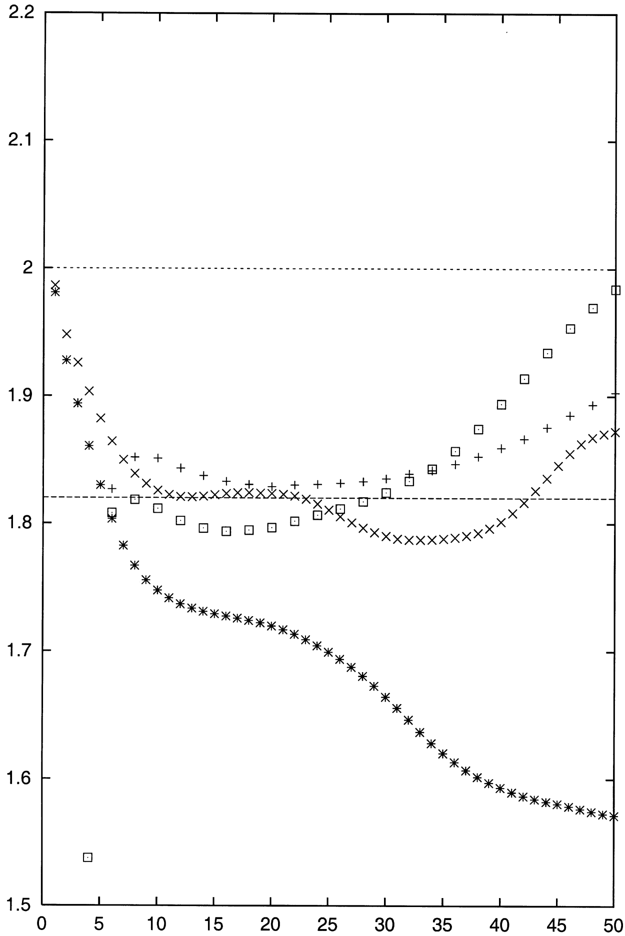

Fig. 5. Logarithmic local slopes of the ESS plot of raw structure function of order 4 versus raw structure function of order 2 at $r_c^z = 64$ ($\times$), at $r_c^z = 32$ ($\bigstar$) and of the $j = 0$ projection centered at $r_c^z = 64$ ($+$), and at $r_c^z = 32\,(\square)$. Also two horizontal lines corresponding to the high Reynolds number limit, 1.82, and to the K41 nonintermittent value, 2, are shown.

possesses a $j = 0$ component will be dominated eventually by an isotropic scaling behavior. But quantities that do not have a $j = 0$ may exhibit anisotropic behaviour on all scales. For example, in hydrodynamic turbulence odd transverse structure function must vanish in the isotropic sector. Nevertheless, they do have contributions corresponding to $\ell \neq 0$. Evidently, their decay with scales will be determined by exponents of $\ell \neq 0$, and they will never be dominated by isotropic scaling behaviour, no matter how small the scale is or how large the Reynolds number is. Thus, one expects that there will be lingering effects of the anisotropic forcing on arbitrarily small scales. It is important and worthwhile to understand this further.

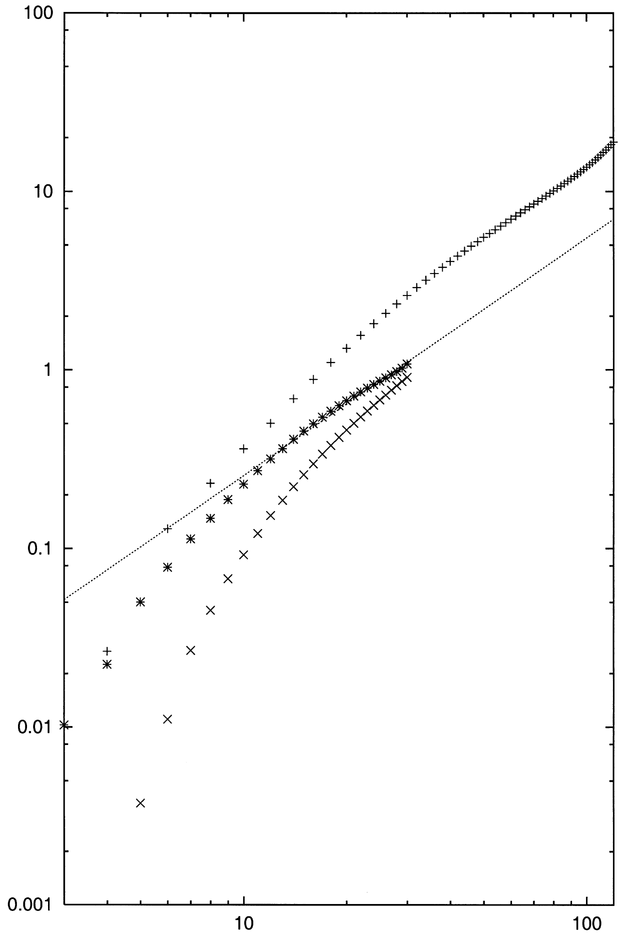

Fig. 6. Log–log plot of $S_{2,22}$ (★); $S_{2,20}$ (×) as functions of R at $r_z^c = 32$ and of $S_{2,2}^{(2)}$ as a function of R (+) at the center, $r_z^c = 64$. The straight line corresponds to the expectation of dimensional analysis: $\zeta_2^{(2)} = \frac{4}{3}$.

Acknowledgements

This work has been supported in part by the Israel Science Foundation administered by the Israel Academy of Sciences and Humanities, the German–Israeli Foundation and the Naftali and Anna Backenroth–Bronicki Fund for Research in Chaos and Complexity.

Appendix A. Construction of constant tensors belonging to irreducible representations of SO(3)

The construction of constant tensors which transform according to the (ℓ, m) sector of SO(3) under rotations, is usually done using the Young tableaux machinery [19].

However, for practical and calculational reasons, we offer a much simpler and straightforward technique. The key point is to take an object that readily transforms according to the (ℓ,m) sector, (i.e., the spherical harmonic $Y_{\ell,m}(\hat{\boldsymbol{u}})$), and to turn it into a constant tensor using *isotropic operations*. By isotropic operations we mean contraction/multiplication with $x^\alpha, \partial^\alpha, \delta^{\alpha\beta}$. The isotropy of these operations ensures that the resulting object will have the same transformation rules under rotation as the original one, therefore belongs to the (ℓ,m) sector of the SO(3) group. A detailed review of this technique is found in Ref. [1].

Consider the constant tensor

$$B^{\alpha_1,\ldots,\alpha_{2n}}_{\ell m,2n} \equiv \partial^{\alpha_1}\cdots\partial^{\alpha_{2n}} u^{2n} Y_{\ell m}(\hat{\boldsymbol{u}}), \quad \ell \leqslant 2n\,. \tag{A.1}$$

By definition, $B^{\alpha_1,\ldots,\alpha_{2n}}_{\ell m,2n}$ is a completely symmetric, constant tensor (does not depend on $\hat{\boldsymbol{u}}$). In addition, it transforms under rotations according to the (ℓ,m) sector for it is composed out of $Y_{\ell m}(\hat{\boldsymbol{u}})$ and isotropic operations. Furthermore, it can be argued that up to an overall constant it is the *only* completely symmetric tensor in the (ℓ,m) sector (a different tensor would imply a different spherical harmonic, with the same (l,m), which is impossible).

The calculations presented in the text are simplified by the use of two identities. The first one is

$$\delta_{\alpha_1\alpha_2} B^{\alpha_1,\ldots,\alpha_{2n}}_{\ell m,2n} = z_{2n,\ell} B^{\alpha_3,\ldots,\alpha_{2n}}_{\ell m,2n-2}\,, \tag{A.2}$$

$$z_{2n,\ell} = [2n(2n+1) - \ell(\ell+1)]\,, \tag{A.3}$$

which is derived by noting that the contraction of $\delta_{\alpha_1\alpha_2}$ with $B^{\alpha_1,\ldots,\alpha_{2n}}_{\ell m,2n}$ gives a Laplacian that acts on the spherical harmonic in the definition of $B^{\alpha_1,\ldots,\alpha_{2n}}_{\ell m,2n}$, and hence the factor $z_{2n,\ell}$. The second one is

$$\sum_{i\neq j} \delta^{\alpha_i\alpha_j} B^{\{\alpha_m\},m\neq i,j}_{\ell m,2n-2} = B^{\alpha_1,\ldots,\alpha_{2n}}_{\ell m,2n}, \quad \ell \leqslant 2n-2\,. \tag{A.4}$$

This identity is proved by writing u^{2n} in (A.1) as $u^2 u^{2n-2}$, and operating with the derivative on u^2. The term obtained as $u^2\partial^{\alpha_1}\ldots\partial^{\alpha_{2n}} u^{2n-2} Y_{\ell m}(\hat{u})$ vanishes because we have $2n$ derivatives on a polynomial of degree $2n-2$.

References

[1] I. Arad, V.S. L'vov, I. Procaccia, Correlation functions in isotropic and anisotropic turbulence: the role of the symmetry group, Phys. Rev. E 59 (1999) 6753.

[2] I. Arad, B. Dhruva, S. Kurien, V.S. L'vov, I. Procaccia, K.R. Sreenivasan, The extraction of anisotropic contributions in turbulent flows, Phys. Rev. Lett. 81 (1998) 5330.

[3] I. Arad, L. Biferale, I. Mazzitelli, I. Procaccia, Disentangling scaling properties in anisotropic and inhomogeneous turbulence, Phys. Rev. Lett. 82 (1999) 5040.

[4] S. Kurien, V.S. L'vov, I. Procaccia, K.R. Sreenivasan, The scaling structure of the velocity statistics in atmospheric boundary layer, Phys. Rev. E, in press.

[5] R.H. Kraichnan, Small-scale structure of passive scalar advected by turbulence, Phys. Fluids 11 (1968) 945.

[6] M. Vergassola, Anomalous scaling for passively advected magnetic fields, Phys. Rev. E 53 (1996) R3021.
[7] K. Gawedzki, A. Kupiainen, Anomalous scaling of the passive scalar, Phys. Rev. Lett. 75 (1995) 3834.
[8] M. Chertkov, G. Falkovich, I. Kolokolov, V. Lebedeev, Normal and anomalous scaling of the fourth-order correlation function of a randomly advected passive scalar, Phys. Rev. E 52 (1995) 4924.
[9] A. Fairhall, O. Gat, V.S. L'vov, I. Procaccia, Anomalous scaling in a model of passive scalar advection: exact results.
[10] A. Lanotte, A. Mazzino, Anisotropic nonperturbative zero modes for passively advected magnetic fields, Phys. Rev. E 60 (1999) R3483.
[11] A. Lanotte, A. Mazzino, Anisotropic nonperturbative zero modes for passively advected magnetic fields, Phys. Rev. E 53 (1996) 3518.
[12] L.Ts. Adzhemyan, N.V. Antonov, A.V. Vasil'ev, Phys. Rev. E 58 (1998) 1823.
[13] I. Arad, V.S. L'vov, E. Podivilov, I. Procaccia, Anomalous scaling in the anisotropic sectors of the Kraichnan model of passive scalar advection, Phys Rev. E, submitted for publication.
[14] I. Arad, L. Biferale, I. Procaccia, Nonperturbative spectrum of anomalous scaling exponents in the anisotropic sectors of passively advected magnetic fields, Phys. Rev. E, in press.
[15] B.I. Shraiman, E.D. Siggia, Lagrangian path integrals and fluctuations of random flows, Phys. Rev. E 49 (1974) 2912.
[16] O. Gat, R. Zeitak, Phys. Rev. E 57 (1998) 5331.
[17] U. Frisch, A. Mazzino, A. Noullez, M. Vergassola, Lagrangian method for multiple correlations in passive scalar advection, Phys. Fluids 11 (1999) 2178, Vergassola Frisch.
[18] O. Gat, I. Procaccia, R. Zeitak, Anomalous scaling in passive scalar advection: Monte-Carlo Lagrangian trajectories, Phys. Rev. Lett. 80 (1998) 5536.
[19] M. Hamermesh, Group Theory and its Applications to Physical Problems, Addison-Wesley, Reading, MA, 1964.
[20] Y. Cohen, V.S. L'vov, A. Pomyalov, I. Procaccia, Scaling exponents in the Kraichnan model for all the parameter range, in preparation.
[21] D. Bernard, K. Gawedcki, A. Kupiainen, Phys. Rev. E 54 (1996) 2624.
[22] G. Amati, R. Benzi, S. Succi, Phys. Rev. E 55 (1997) 6985.
[23] F. Toschi, G. Amati, S. Succi, R. Benzi, R. Piva, Intermittency of structure functions on channel flow turbulence, Phys. Rev. Lett. (1998), submitted for publication.
[24] G. Amati, S. Succi, R. Piva, Int. J. Mod. Phys. C 8 (1997) 869.
[25] V. Borue, S.A. Orszag, J. Fluid. Mech. 306 (1996) 293.
[26] S.G. Saddoughi, S.V. Veeravalli, J. Fluid. Mech. 268 (1994) 333.
[27] E. Gaudin, B. Protas, S. Gouion-Durand, J. Wojciechowski, J.E. Wesfried, Phys. Rev. E 57 (1998) R9.
[28] R. Benzi, S. Ciliberto, R. Tripiccione, C. Baudet, F. Massaioli, S. Succi, Phys. Rev. E 48 (1993) R29.